Opposing Effects of Inositol Hexakisphosphate on Rod Arrestin and Arrestin2 Self-Association†

Susan M. Hanson,‡,§ Sergey A. Vishnivetskiy,‡ Wayne L. Hubbell,*,|| and Vsevolod V. Gurevich*,‡

Department of Pharmacology, Vanderbilt University School of Medicine, Nashville, Tennessee 37232, and Jules Stein Eye Institute and Department of Chemistry and Biochemistry, University of California, Los Angeles, Los Angeles, California 90095

Received October 23, 2007; Revised Manuscript Received November 19, 2007

ABSTRACT: The robust cooperative formation of rod arrestin tetramers has been well-established, whereas the ability of other members of the arrestin family to self-associate remains controversial. Here, we used purified arrestins and multi-angle light scattering to quantitatively compare the propensity of the four mammalian arrestin subtypes to self-associate. Both non-visual and cone arrestins only form oligomers at very high non-physiological concentrations. However, inositol hexakisphosphate (IP6), a fairly abundant form of inositol in the cytoplasm, greatly facilitates self-association of arrestin2. Arrestin2 self-association equilibrium constants in the presence of 100 μM IP6 suggest that an appreciable proportion could exist in an oligomeric state but only in intracellular compartments where its concentration is 5−10-fold higher than average. In contrast to arrestin2, IP6 inhibits self-association of rod arrestin, indicating that the structure of these two tetramers in solution is likely different.

Arrestins are multi-functional adaptor proteins that regulate signaling of G protein-coupled receptor (GPCR)[1]-dependent and -independent pathways. The first discovered and most studied function of arrestins is their ability to terminate GPCR signaling by preferentially binding the activated phosphorylated form of the receptor (reviewed in refs *1* and *2*). There are four types of mammalian arrestins. The two subtypes expressed in photoreceptor cells, termed rod and cone arrestin, terminate rhodopsin and cone opsin signaling, respectively. The two non-visual subtypes, arrestins2 and -3 (i.e., β-arrestins1 and -2), are expressed ubiquitously and bind hundreds of different GPCRs (reviewed in ref *3*). Arrestins also interact with numerous non-receptor binding partners including clathrin (*4*) and AP2 (*5*) to orchestrate intracellular trafficking of the arrestin−receptor complex, as well as members of the MAPK kinase cascades (cRaf, ERK1/2, ASK, and JNK3) (*6*−*9*), Src family kinases (*10*), the ubiquitin ligase Mdm2 (*8*, *9*, *11*, *12*), calmodulin (*13*), microtubules (*14*, *15*), and phosphoinositides (*16*−*18*).

The crystal structures of bovine rod arrestin, arrestin2, and salamander cone arrestin are strikingly similar (*19*−*22*). Detectable differences in the structures are limited to several loops, where similar variations exist in different crystal forms of the same protein (*19*, *20*). Biologically, however, rod arrestin is unique. It is the only member of the arrestin family designed to bind just one receptor, rhodopsin. The concentration of rod arrestin in photoreceptors (>1 mM) (*23*−*25*) exceeds the level of other arrestin subtypes in all cell types by several 100-fold (*26*, *27*). It is also the only arrestin that invariably crystallizes as a tetramer (*19*, *28*), suggesting that self-association may be a unique feature of rod arrestin. Rod arrestin forms tetramers at physiological concentrations according to the following model: 2M ↔ D (K_1) and 2D ↔ T (K_2), where M, D, and T are monomer, dimer, and tetramer, respectively (MDT model). Its self-association constants indicate that the tetramer form of arrestin likely predominates in rods (*29*, *30*). The role of rod arrestin self-association is not entirely clear. A dramatic light-dependent redistribution of arrestin in rod photoreceptors (*23*, *31*), along with the ability of the tetramer to bind microtubules (the default low-affinity arrestin partner in dark-adapted photoreceptors) but not light-activated rhodopsin (its high-affinity binding partner in the light) (*29*), suggests that reversible tetramer formation may play a role in the appropriate subcellular localization of arrestin and regulate its availability for light-activated rhodopsin and possibly other interaction partners.

Recent studies suggest that both non-visual arrestins may also form oligomers in cells (*32*, *33*) and that their self-association depends on their interaction with inositol hexakisphosphate (IP6) (*32*). IP6 is the most abundant inositol polyphosphate in many cell types (reaching concentrations of 100 μM) (*34*, *35*). It is believed to play a role in numerous cellular events including receptor trafficking, neurotransmission, ion channel activation, mRNA export, etc. (reviewed in refs *35* and *36*). Rod and both non-visual arrestins bind IP6, albeit with very different affinities (*18*). Here, we use multi-angle laser light

† This work was supported by NIH Grants EY11500 (V.V.G.) and EY05216 and the Jules Stein Professorship Endowment (W.L.H.). S.M.H. was supported by Training Grant GM07628.

* Corresponding authors. (W.L.H.) Tel.: (310) 206-8830; fax: (310) 792-2144; e-mail: hubbellw@jsei.ucla.edu. (V.V.G.) Tel.: (615) 322-7070; fax: (615) 343-6532; e-mail: vsevolod.gurevich@vanderbilt.edu.

‡ Vanderbilt University School of Medicine.

§ Current address: University of Wisconsin−Madison, Department of Physiology, 601 Science Dr., Madison, WI 53711.

|| University of California, Los Angeles.

[1] Abbreviations: IP6, inositol hexakisphosphate; GPCR, G protein-coupled receptor; K_{Ddim}, monomer−dimer equilibrium dissociation constant; K_{Dtet}, dimer−tetramer equilibrium dissociation constant; CLArr2, cysteine-less arrestin2.

10.1021/bi7021359 CCC: $40.75
Published on Web 12/28/2007

scattering to determine the ability of different arrestin subtypes to oligomerize and show that the self-association of rod arrestin and arrestin2 is differentially affected by IP6. Our findings demonstrate that arrestins2 and -3 and cone arrestin do not self-associate at physiologically relevant concentrations in the absence of IP6. In the presence of IP6, arrestin2 self-association is dramatically enhanced, although the affinity of this interaction suggests that oligomerized arrestin2 in cells can only exist in compartments with unusually high local arrestin concentrations.

EXPERIMENTAL PROCEDURES

Arrestin Expression and Purification. Arrestin was expressed in *Escherichia coli* and purified as described (*37*). The substituting residues for the native cysteines in the cysteine-less arrestin2 mutant, CLArr2 (C59V, C125S, C140L, C150V, C242V, C251V, and C269S), were selected based on the highest resolution crystal structure available (*20*) to avoid clashes and to maximally preserve intramolecular interactions. This arrestin is fully functional in terms of receptor (*13*, *15*), calmodulin (*13*), and microtubule binding (*15*) and is expressed in *E. coli* essentially as well as wild-type arrestin.

Light Scattering. All light scattering measurements were made with a DAWN EOS detector coupled to an Optilab refractometer (Wyatt Technologies) following gel filtration on a 7.8 mm (i.d.) × 15.0 cm (length) QC-PAK GFC 300 column (Tosoh Bioscience). The arrestin samples (100 μL) at different concentrations were injected onto the column at 25 °C, at a flow rate of 0.8 mL/min in 50 mM MOPS, 100 mM NaCl, pH 7.2 with or without 100 μM IP6. The column used did not resolve oligomeric species but simply acted as a filter to remove highly scattering particulates. Light scattering at 18 angles (15−160°), absorbance at 280 nm, and the refractive index (at 690 nm) for each sample were taken for a narrow slice at the peak of the elution profile (*38*).

The model for oligomer formation (MDT) is that given by Imamoto et al. (*30*)

$$2\mathrm{M} \leftrightarrow \mathrm{D}\ (K_1)$$

$$2\mathrm{D} \leftrightarrow \mathrm{T}\ (K_2)$$

The relationships describing the arrestin equilibria according to this model are

$$K_1 = \frac{\mathrm{D}}{\mathrm{M}^2} \quad K_2 = \frac{\mathrm{T}}{\mathrm{D}^2} \quad \mathrm{M} + 2\mathrm{D} + 4\mathrm{T} = C$$

where M, D, and T are the monomer, dimer, and tetramer concentrations, respectively, and C is the total protein concentration. From these relationships and particular values for K_1, K_2, and C, the concentrations of monomer, dimer, and tetramer may be obtained as solutions to eqs 1−3

$$\mathrm{M} + 2K_1\mathrm{M}^2 + 4K_1{}^2K_2\mathrm{M}^4 - C = 0 \qquad (1)$$

$$\mathrm{D} = K_1\mathrm{M}^2 \qquad (2)$$

$$\mathrm{T} = \mathrm{D}^2K_2 = K_1{}^2K_2\mathrm{M}^4 \qquad (3)$$

Using the values of M, D, and T thus determined, the weight-average molecular weight is computed as

$$\mathrm{MW}_{\mathrm{av}} = M_{\mathrm{m}}\frac{(\mathrm{M} + 4\mathrm{D} + 16\mathrm{T})}{\mathrm{M} + 2\mathrm{D} + 4\mathrm{T}} \qquad (4)$$

where M_{m} is the monomer molecular weight (M_{m} = 45 000, 46 000, 45 500, and 43 000 for rod arrestin, arrestin2, arrestin3, and cone arrestin, respectively).

The value for C in the light scattering cell at the point where data were collected was determined from the refractive index increment (0.184 g/mL) and A_{280}, both of which were in agreement. The experimental $\mathrm{MW}_{\mathrm{av}}$ values were then obtained from the concentration and light scattering data using Astra for Windows 4.90 software (Wyatt Technologies). Experimental data for $\mathrm{MW}_{\mathrm{av}}$ as a function of C were least-squares fit to eqs 1−4 with only K_1 and K_2 as adjustable parameters. The probable error associated with any given $\mathrm{MW}_{\mathrm{av}}$ point was taken as the standard deviation of the best fit from the extensive data for wild-type rod arrestin (±1000). Errors in K_1 and K_2 for the other arrestins were determined using this value and the least-squares fit. Estimated errors for the reported K_{D} values (dissociation constants) did not exceed 15%.

RESULTS

Only Rod Arrestin Self-Associates at Physiologically Relevant Concentrations. The arrestin monomer has two domains, each containing a seven-stranded β sandwich at its core. Rod arrestin invariably crystallizes as a tetramer (dimer of dimers), where two nearly identical conformations of monomer, which differ only in three discrete plastic loop regions, form each dimer (*19*, *28*). Although rod arrestin forms tetramers under normal physiological conditions in solution, the structure of the solution tetramer is different from the crystal form (*29*). The formation of the rod arrestin tetramer is well-described by the MDT model. It is cooperative (i.e., the dissociation constant for the dimer−tetramer equilibrium (K_{Dtet}) (7.5 μM) is lower than the dissociation constant for the monomer−dimer equilibrium (K_{Ddim}) (36.8 μM) (*29*, *30*)). In contrast, arrestin2 and cone arrestin crystallize as monomers (*20*−*22*), suggesting that self-association may be a special feature of rod arrestin. To test this hypothesis, we compared the self-association of purified bovine rod arrestin, arrestin2, arrestin3, and human cone arrestin using multi-angle laser light scattering (Figure 1A). This method provides the weight-average molecular weight of a self-associating protein in solution and has been successfully employed to study protein−protein association by several groups (*29*, *38*, *39*).

Analysis of the light scattering data reveals that rod arrestin has the highest propensity to self-associate (Figure 1A). In contrast, arrestin2, its functionally equivalent cysteine-less mutant (CLArr2) (*13*, *15*), arrestin3, and cone arrestin all show relatively weak self-association (Figure 1A). For each arrestin species (except rod arrestin), the data can be well fit to a simple monomer−dimer equilibrium, although the formation of tetramers at higher concentrations cannot be excluded based on the limited concentration range explored. For arrestin2, CLArr2, and arrestin3, the K_{D} value for the

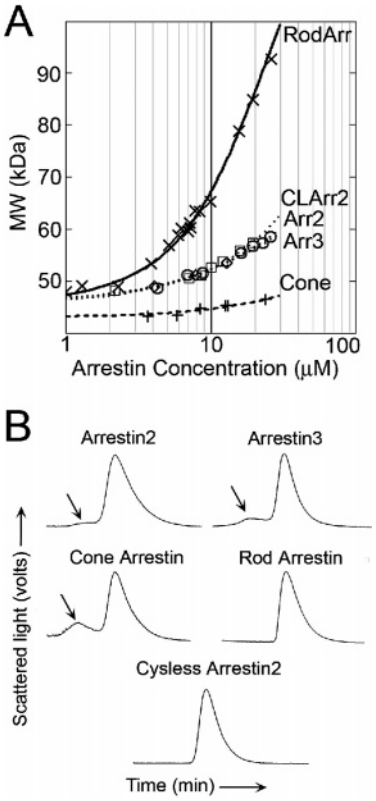

FIGURE 1: Cone and non-visual arrestins do not self-associate at physiological concentrations. (A) Weight-average molecular weight of arrestin2 (Arr2; circles), arrestin3 (Arr3; diamonds), cone arrestin (Cone; +), and cysteine-less arrestin2 (CLArr2; squares) at various concentrations was determined from the light scattering data as described in the Experimental Procedures and compared to rod arrestin (RodArr; ×). The curves are fits to the MDT model obtained as described in the Experimental Procedures. (B) Elution profiles (scattered light vs time) of each arrestin subtype. Arrestins2 and -3 and cone arrestin show a small, higher MW peak corresponding to dimers (arrows) that elutes prior to the main arrestin peak.

monomer−dimer equilibrium (K_{Ddim}) derived from the fits is in the range of 98−110 μM; for cone arrestin, it is ≈500 μM.

The equilibrium constants for rod arrestin self-association and its concentration in photoreceptors (>1 mM) (*23*−*25*) suggest that the tetramer is likely the predominant form in vivo (*29*). In contrast, the intracellular concentrations of cone arrestin, arrestin2, and arrestin3 are only ∼4 μM (*27*), 0.03−0.2 μM, and 0.01−0.03 μM (*26*), respectively. Even in types of neurons where arrestin2 is predominantly nuclear (*8*), its concentration in this compartment is unlikely to exceed 2 μM. Thus, for non-visual and cone arrestins, the proportion of oligomer present in cells would be negligible (<1%) without extremely high local concentrations and/or other binding partners that enhance their self-association.

Initially, we found that the elution profiles of cone and the non-visual arrestins from a size exclusion column (detected by light scattering) were different from that of rod arrestin. In addition to the main protein peak, where the average molecular weight varied as a function of concentration, we observed a smaller peak representing a higher MW species roughly twice the size (∼100 kDa) of the monomer (Figure 1B). Interestingly, the proportion of the protein in the higher MW peak typically represented <2% of the total arrestin in the experiment and did not correlate with the total arrestin concentration. Arrestin2 has a number of exposed cysteine residues (four out of seven) (*20*, *22*). Assuming that arrestin3 and human cone arrestin have a similar structure, six out of nine and six out of eight cysteines, respectively, in these proteins would also be exposed, in contrast to rod arrestin, which has only one exposed cysteine (*19*). Conceivably, the observed higher MW peak represents a dimer cross-linked via exposed cysteines. To test this hypothesis, we performed the same experiments on CLArr2, a purified fully functional version of arrestin2 that had all of its cysteines replaced (C59V, C125S, C140L, C150V, C242V, C251V, and C269S). Unlike cone and the non-visual arrestins but similar to rod arrestin, CLArr2 had only one major scattering peak, which rose sharply and eventually trailed off (Figure 1B). These data demonstrate that the higher MW peak was the result of intermolecular cross-linking between sulfhydryl groups in these arrestins. This type of dimerization is extremely unlikely in the reducing intracellular environment. Therefore, it probably does not represent a physiologically relevant mode of arrestin self-association.

IP6 Differentially Affects Rod Arrestin and Arrestin2 Self-Association. Several groups have demonstrated that rod arrestin and arrestins2 and -3 bind IP6 (*16*−*18*, *32*, *40*). This interaction inhibits arrestin binding to rhodopsin (*16*, *40*). Phosphoinositide interaction (via the same site where IP6 binds) may be involved in the light-dependent trafficking of *Drosophila* visual arrestins (*17*, *41*) and non-visual arrestin-dependent receptor internalization (*18*). A recent study by Milano et al. also suggests that IP6 enhances the oligomerization of non-visual arrestins (*32*). Intracellular concentrations of IP6 are believed to range from 37 to 105 μM (*34*). Therefore, we tested the effect of IP6 directly by comparing the self-association of rod arrestin and arrestin2 in the presence and absence of 100 μM IP6. At this concentration, IP6 dramatically enhanced the ability of arrestin2 to form oligomers (Figure 2A). In the presence of IP6, the best fits to the light scattering data were obtained according to the MDT model: $K_{Ddim} \approx 12$ μM and $K_{Dtet} \approx 2$ μM, values significantly smaller than those for rod arrestin. Enhancement of self-association in the presence of IP6 was also observed with CLArr2, although the effect was less dramatic (Figure 2A). In this case, fits to the MDT model gave $K_{Ddim} \approx 58$ μM and $K_{Dtet} \approx 14$ μM. In neither case could the data be satisfactorily fit to a simple monomer−dimer equilibrium. Estimation of the percentage of oligomeric arrestin2 at its measured intracellular concentrations (∼0.2 μM) suggests that even with its self-association dramatically enhanced by IP6, a maximum of only ∼3% of arrestin2 would be oligomerized in cells (Figure 2B). Even when the local concentration is 10 times higher (∼2 μM), no more than 25% of arrestin2 would self-associate in the presence of IP6. In contrast, we found that IP6 inhibits self-association of rod arrestin (Figure 2A). However, the values of K_{Ddim} (≈120 μM) and K_{Dtet} (≈18 μM) in the presence of 100 μM IP6 indicate that rod arrestin oligomers (dimer plus tetramer) would still predominate in rod photoreceptors (Figure 2B).

DISCUSSION

Although arrestin self-association was discovered in 1977 (*42*), investigation of this phenomenon started only after two independent reports showed that rod arrestin crystallizes as a tetramer (*19*, *28*). An early study using sedimentation

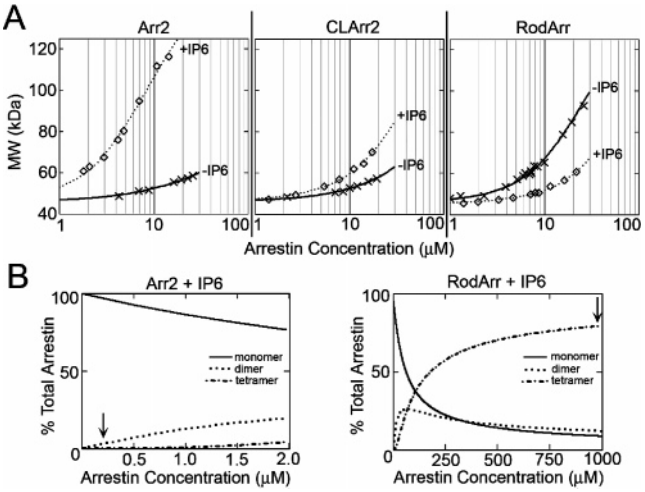

FIGURE 2: IP6 differentially affects rod and arrestin2 self-association. (A) Weight-average molecular weight of arrestin2 (Arr2), cys-less arrestin2 (CLArr2), and rod arrestin (RodArr) at various concentrations in the presence (diamonds) and absence (×) of 100 μM IP6 was determined by light scattering as described in the Experimental Procedures. The curves are fits to the MDT model obtained as described in the Experimental Procedures. (B) Distribution of monomer (solid line), dimer (dotted line), and tetramer (dotted−dashed line) as a function of concentration was calculated based on the estimated equilibrium constants in the presence of 100 μM IP6 at 25 °C for arrestin2 ($K_{Ddim} \approx 11.8$ μM and $K_{Dtet} \approx 1.9$ μM) (left panel) and rod arrestin ($K_{Ddim} \approx 120$ μM and $K_{Dtet} \approx 18.1$ μM) (right panel). Note the difference in scale of the *x*-axis. Arrows indicate the estimated endogenous concentration of arrestin2 in mature neurons (*26*) and rod arrestin in rods (*23*−*25*).

equilibrium found that rod arrestin forms dimers and tetramers at physiologically relevant concentrations in solution (*43*). Recently, we used multi-angle laser light scattering to definitively show that rod arrestin cooperatively forms tetramers at physiological concentrations (Figure 1) (*29*), confirming the results of Imamoto et al., who came to the same conclusion using small-angle X-ray scattering (*30*). Considering the equilibrium dissociation constants and the extremely high concentrations of endogenous rod arrestin in photoreceptors (>1 mM) (*23*−*25*), the majority of arrestin is likely oligomeric in vivo, although the function of its self-association has not been unambiguously established. In rods, arrestin moves between compartments of the cell in a light-dependent manner. This movement is thought to contribute to light adaptation (*24*, *44*) and is believed to involve high-affinity binding of arrestin to activated rhodopsin in the outer segments in the light and low-affinity interaction with microtubules in the inner segments in the dark (*31*). We recently demonstrated that the tetrameric form of rod arrestin is capable of binding microtubules but that only monomeric arrestin binds light-activated rhodopsin (*29*). These data suggest that the tetramer is a storage form and that self-association increases the arrestin-binding capacity of microtubules in dark-adapted photoreceptors.

Unlike rod arrestin, cone arrestin and arrestin2 crystallize as monomers (*20*−*22*). However, the high homology between arrestin subtypes (*21*) and data suggesting that arrestins2 and -3 oligomerize in cells (*32*, *33*) prompted us to test whether cone arrestin and the two ubiquitous non-visual arrestins self-associate in solution. We found that all three subtypes show a certain propensity to self-associate (Figure 1A). Arrestins2 and -3 each have $K_{Ddim} = \sim 100$ μM, whereas cone arrestin has only a minimal tendency to self-associate ($K_{Ddim} \approx 500$ μM). Thus, association of these arrestins does not appear to be physiologically relevant since their concentrations are relatively low (0.01−4 μM) in cells that express these arrestin subtypes (*26*, *27*).

Arrestin interaction with IP6 was discovered over 25 years ago (*16*) and has since been characterized by several groups. Rod arrestin has a low-affinity IP6 binding site in the arrestin N-domain ($K_D = 5-18$ μM) (*16*, *18*) in the same part of the molecule that binds receptor-attached phosphates (reviewed in ref *2*). This explains why IP6 inhibits the arrestin−rhodopsin interaction (*16*, *40*). In contrast, arrestins2 and -3 bind IP6 with a higher affinity ($K_D = \sim 85$ nM) via a second binding site localized on the concave surface of the C-domain (*18*, *32*). IP6 binding sites in arrestin2 were extensively studied by crystallography and mutagenesis (*32*). On the basis of the arrestin2−IP6 crystal lattice, in which IP6 is sandwiched in between the N-domain of one arrestin molecule and the C-domain of another in an extended chain, the authors proposed that IP6 may induce oligomer formation and showed experimentally that arrestin2 and -3 oligomerization is in fact enhanced by IP6 in solution. To determine the extent of this effect directly, we measured the self-association equilibrium constants of arrestin2 in the presence of IP6 using light scattering. In agreement with previous findings, our results indicate that arrestin2 self-association is dramatically enhanced by IP6 (Figure 2). We also found that whereas arrestin2 primarily forms dimers in the absence of IP6, it forms tetramers in a cooperative manner in the presence of IP6.

Importantly, this cooperativity means that the interaction energy of tetramer formation is greater than that of dimer formation, implying a greater area of contact between the two dimers than between two monomers in a dimer. This is more likely to be the case if the solution tetramer has a closed circular configuration, in which each arrestin molecule would interact with two sister subunits. By soaking preformed crystals of arrestin2 monomers (*22*) with IP6, Milano et al. observed open extended chains of arrestin molecules (*32*) that cannot account for cooperativity because in this configuration, all arrestin−arrestin interactions are exactly the same (*32*). The mutagenesis data presented by Milano et al. (*32*) support the localization of IP6 binding sites observed in these crystals, but their data in solution show the formation of a few distinct forms rather than a heterogeneous mix of multiple oligomeric species that an open chain configuration predicts (*32*). Importantly, the orientation of arrestin2 molecules relative to one another was fixed by crystallization in the absence of IP6, so that the structure of the arrestin2 oligomer in these crystals does not necessarily reflect that which exists in solution. For example, we recently demonstrated that this is the case for rod arrestin: the open tetramer structure observed in the crystal is dramatically different from the actual shape of the solution tetramer (*29*). The opposite effects of IP6 on the self-association of rod arrestin and arrestin2 (Figure 2) suggest that the orientation of the monomers and/or contact interfaces between them in the tetramers of these arrestin subtypes are likely different.

Regardless of their structure, the formation of non-visual arrestin oligomers in cells can only occur locally where their concentration is elevated many fold, even when the dramatic effect of IP6 is taken into account. This appears to be at

odds with several studies asserting that arrestins2 and -3 self-associate in cells. Storez et al. (*33*) using BRET/FRET and co-immunoprecipitation reported oligomer formation of overexpressed tagged arrestins. Milano et al. (*32*) also detected oligomers by co-immunoprecipitation and showed that overexpression of arrestin mutants that cannot bind IP6 (and therefore do not oligomerize) alters the subcellular localization of arrestin. In addition, recent proteomics analysis in cells overexpressing arrestin2 or -3 suggests that the two non-visual arrestins interact with each other and possibly with rod arrestin (*45*). However, all these methods have several important caveats. First, the level of arrestin overexpression was not quantified. Using quantitative Western blot analysis with the appropriate calibration curves, we found that similar expression constructs yield 40−100 pmol/mg of non-visual arrestins (*8*, *9*), which translates into ∼4−10 μM arrestin in cells. These concentrations approach the equilibrium self-association constants measured for arrestin2 in the presence of IP6 (Figure 2), but they exceed the maximum level of endogenous arrestin2 and -3 expression by 20−50 and >100 times, respectively (*26*). Thus, one must be wary of using overexpressed proteins to study a phenomenon that is critically dependent on concentration. Second, co-immunoprecipitation can demonstrate the existence of protein complexes, but without appropriate quantification, it is impossible to judge whether a significant proportion of these proteins interacts. In our experience, protein−protein complexes can be easily detected when no more than 1% of either partner is associated with the other (*13*, *15*). Third, the addition of large (>20 kDa) tags such as luciferase and fluorescent proteins to arrestins dramatically changes their intracellular distribution (*8*, *9*). Therefore, the biological relevance of the observed homo- and hetero-oligomerization of overexpressed non-visual arrestins remains to be elucidated.

The effect of IP6 on rod arrestin self-association (increase in K_{Ddim} from 37 to 120 μM and K_{Dtet} from 7.5 to 18 μM) (Figure 2 and ref *29*) may be physiologically relevant. Conceivably, IP6 may modulate the oligomeric equilibrium of arrestin in rods to maintain a certain level of monomer to rapidly quench rhodopsin signaling. However, unless the concentration of IP6 in rod photoreceptors is much higher than in other cells (where it reaches up to 100 μM (*34*, *35*)), rods would contain a much higher concentration of arrestin than IP6, limiting the possible impact of IP6 on rod arrestin self-association status. On the other hand, since the concentration of rod arrestin is so high in photoreceptors (>1 mM) (*23*−*25*), its binding to IP6, even with relatively low affinity, might serve to scavenge free IP6, thereby reducing its concentration. Since micromolar concentrations of free IP6 inhibit arrestin binding to light-activated phosphorhodopsin (*16*, *40*), this effect may be biologically relevant.

Interestingly, whereas rod arrestin has the highest, cone arrestin has the lowest propensity to self-associate (Figure 1). Apparently, its relatively low concentration in cones (*27*) makes this robust storage mechanism unnecessary.

Mapped IP6 binding sites localize on the concave surfaces of the two arrestin domains (*17*, *18*, *32*). GPCRs (*46*−*48*), microtubules (*14*, *15*), and calmodulin (*13*) all bind to the same arrestin surface, suggesting that these partners could compete with IP6. The affinity of arrestins for their cognate receptors is subnanomolar (*49*, *50*), so that IP6 even at 100 μM does not significantly inhibit receptor binding (*16*, *40*). On the other hand, arrestin affinity for microtubules and calmodulin is in the micromolar range (*13*−*15*), so that IP6 may regulate its interaction with these partners. In summary, although IP6 has the potential to facilitate the self-association of non-visual arrestins under special circumstances in cellular compartments where these proteins are highly concentrated, it may also regulate other functions of all arrestin proteins, such as their interactions with the cytoskeleton and/or with calmodulin, the most ubiquitous regulator of Ca^{2+}-dependent processes in the cell.

ACKNOWLEDGMENT

The authors are grateful to Cherie Hubbell for technical assistance and Dr. Christian Altenbach for help with data analysis.

REFERENCES

1. Carman, C. V., and Benovic, J. L. (1998) G-protein-coupled receptors: Turn-ons and turn-offs, *Curr. Opin. Neurobiol. 8*, 335−344.
2. Gurevich, V. V., and Gurevich, E. V. (2004) The molecular acrobatics of arrestin activation, *Trends Pharmacol. Sci. 25*, 105−112.
3. Gurevich, V. V., and Gurevich, E. V. (2006) The structural basis of arrestin-mediated regulation of G protein-coupled receptors, *Pharmacol. Ther. 110*, 465−502.
4. Goodman, O. B., Jr., Krupnick, J. G., Santini, F., Gurevich, V. V., Penn, R. B., Gagnon, A. W., Keen, J. H., and Benovic, J. L. (1996) Beta-arrestin acts as a clathrin adaptor in endocytosis of the beta2-adrenergic receptor, *Nature (London, U.K.) 383*, 447−450.
5. Laporte, S. A., Oakley, R. H., Zhang, J., Holt, J. A., Ferguson, S. S., Caron, M. G., and Barak, L. S. (1999) The β2-adrenergic receptor/β-arrestin complex recruits the clathrin adaptor AP-2 during endocytosis, *Proc. Natl. Acad. Sci. U.S.A. 96*, 3712−3717.
6. Luttrell, L. M., Roudabush, F. L., Choy, E. W., Miller, W. E., Field, M. E., Pierce, K. L., and Lefkowitz, R. J. (2001) Activation and targeting of extracellular signal-regulated kinases by beta-arrestin scaffolds, *Proc. Natl. Acad. Sci. U.S.A. 98*, 2449−2459.
7. McDonald, P. H., Chow, C. W., Miller, W. E., Laporte, S. A., Field, M. E., Lin, F. T., Davis, R. J., and Lefkowitz, R. J. (2000) Beta-arrestin 2: A receptor-regulated MAPK scaffold for the activation of JNK3, *Science (Washington, DC, U.S.) 290*, 1574−1577.
8. Song, X., Raman, D., Gurevich, E. V., Vishnivetskiy, S. A., and Gurevich, V. V. (2006) Visual and both non-visual arrestins in their "inactive" conformation bind JNK3 and Mdm2 and relocalize them from the nucleus to the cytoplasm, *J. Biol. Chem. 281*, 21491−21499.
9. Song, X., Gurevich, E. V., and Gurevich, V. V. (2007) Cone arrestin binding to JNK3 and Mdm2: Conformational preference and localization of interaction sites. *J. Neurochem. 103*, 1053−1062.
10. Luttrell, L. M., Ferguson, S. S., Daaka, Y., Miller, W. E., Maudsley, S., Della Rocca, G. J., Lin, F., Kawakatsu, H., Owada, K., Luttrell, D. K., Caron, M. G., and Lefkowitz, R. J. (1999) Beta-arrestin-dependent formation of beta2 adrenergic receptor-Src protein kinase complexes, *Science (Washington, DC, U.S.) 283*, 655−661.
11. Shenoy, S. K., McDonald, P. H., Kohout, T. A., and Lefkowitz, R. J. (2001) Regulation of receptor fate by ubiquitination of activated beta 2-adrenergic receptor and beta-arrestin, *Science (Washington, DC, U.S.) 294*, 1307−1313.
12. Wang, P., Gao, H., Ni, Y., Wang, B., Wu, Y., Ji, L., Qin, L., Ma, L., and Pei, G. (2003) Beta-arrestin 2 functions as a G-protein-coupled receptor-activated regulator of oncoprotein Mdm2, *J. Biol. Chem. 278*, 6363−6370.
13. Wu, N., Hanson, S. M., Francis, D. J., Vishnivetskiy, S. A., Thibonnier, M., Klug, C. S., Shoham, M., and Gurevich, V. V. (2006) Arrestin binding to calmodulin: A direct interaction between two ubiquitous signaling proteins. *J. Mol. Biol. 364*, 955−963.

14. Hanson, S. M., Francis, D. J., Vishnivetskiy, S. A., Klug, C. S., and Gurevich, V. V. (2006) Visual arrestin binding to microtubules involves a distinct conformational change. *J. Biol. Chem. 281*, 9765−9772.
15. Hanson, S. M., Cleghorn, W. M., Francis, D. J., Vishnivetskiy, S. A., Raman, D., Song, X., Nair, K. S., Slepak, V. Z., Klug, C. S., and Gurevich, V. V. (2007) Arrestin mobilizes signaling proteins to the cytoskeleton and redirects their activity. *J. Mol. Biol. 368*, 375−387.
16. Palczewski, K., Pulvermuller, A., Buczylko, J., Gutmann, C., and Hofmann, K. P. (1991) Binding of inositol phosphates to arrestin. *FEBS Lett. 295*, 195−199.
17. Lee, S. J., Xu, H., Kang, L. W., Amzel, L. M., and Montell, C. (2003) Light adaptation through phosphoinositide-regulated translocation of *Drosophila* visual arrestin, *Neuron 39*, 121−132.
18. Gaidarov, I., Krupnick, J. G., Falck, J. R., Benovic, J. L., and Keen, J. H. (1999) Arrestin function in G protein-coupled receptor endocytosis requires phosphoinositide binding, *EMBO J. 18*, 871−881.
19. Hirsch, J. A., Schubert, C., Gurevich, V. V., and Sigler, P. B. (1999) The 2.8 Å crystal structure of visual arrestin: A model for arrestin's regulation, *Cell 97*, 257−269.
20. Han, M., Gurevich, V. V., Vishnivetskiy, S. A., Sigler, P. B., and Schubert, C. (2001) Crystal structure of beta-arrestin at 1.9 Å: Possible mechanism of receptor binding and membrane translocation, *Structure 9*, 869−880.
21. Sutton, R. B., Vishnivetskiy, S. A., Robert, J., Hanson, S. M., Raman, D., Knox, B. E., Kono, M., Navarro, J., and Gurevich, V. V. (2005) Crystal structure of cone arrestin at 2.3 Å: Evolution of receptor specificity. *J. Mol. Biol. 354*, 1069−1080.
22. Milano, S. K., Pace, H. C., Kim, Y. M., Brenner, C., and Benovic, J. L. (2002) Scaffolding functions of arrestin-2 revealed by crystal structure and mutagenesis, *Biochemistry 41*, 3321−3328.
23. Broekhuyse, R. M., Tolhuizen, E. F., Janssen, A. P., and Winkens, H. J. (1985) Light induced shift and binding of *S*-antigen in retinal rods, *Curr. Eye Res. 4*, 613−618.
24. Strissel, K. J., Sokolov, M., Trieu, L. H., and Arshavsky, V. Y. (2006) Arrestin translocation is induced at a critical threshold of visual signaling and is superstoichiometric to bleached rhodopsin, *J. Neurosci. 26*, 1146−1153.
25. Hanson, S. M., Gurevich, E. V., Vishnivetskiy, S. A., Ahmed, M. R., Song, X., and Gurevich, V. V. (2007) Each rhodopsin molecule binds its own arrestin, *Proc. Natl. Acad. Sci. U.S.A. 104*, 3125−3128.
26. Gurevich, E. V., Benovic, J. L., and Gurevich, V. V. (2004) Arrestin2 expression selectively increases during neural differentiation, *J. Neurochem. 91*, 1404−1416.
27. Chan, S., Rubin, W. W., Mendez, A., Liu, X., Song, X., Hanson, S. M., Craft, C. M., Gurevich, V. V., Burns, M. E., and Chen, J. (2007) Functional comparisons of visual arrestins in rod photoreceptors of transgenic mice, *Invest. Ophthalmol. Vis. Sci. 48*, 1968−1975.
28. Granzin, J., Wilden, U., Choe, H. W., Labahn, J., Krafft, B., and Buldt, G. (1998) X-ray crystal structure of arrestin from bovine rod outer segments, *Nature (London, U.K.) 391*, 918−921.
29. Hanson, S. M., Van Eps, N., Francis, D. J., Altenbach, C., Vishnivetskiy, S. A., Arshavsky, V. Y., Klug, C. S., Hubbell, W. L., and Gurevich, V. V. (2007) Structure and function of the visual arrestin oligomer, *EMBO J. 26*, 1726−1736.
30. Imamoto, Y., Tamura, C., Kamikubo, H., and Kataoka, M. (2003) Concentration-dependent tetramerization of bovine visual arrestin, *Biophys. J. 85*, 1186−1195.
31. Nair, K. S., Hanson, S. M., Mendez, A., Gurevich, E. V., Kennedy, M. J., Shestopalov, V. I., Vishnivetskiy, S. A., Chen, J., Hurley, J. B., Gurevich, V. V., and Slepak, V. Z. (2005) Light-dependent redistribution of arrestin in vertebrate rods is an energy-independent process governed by protein−protein interactions, *Neuron 46*, 555−567.
32. Milano, S. K., Kim, Y.-M., Stefano, F. P., Benovic, J. L., and Brenner, C. (2006) Nonvisual arrestin oligomerization and cellular localization are regulated by inositol hexakisphosphate binding, *J. Biol. Chem. 281*, 9812−9823.
33. Storez, H., Scott, M. G. H., Issafras, H., Burtey, A., Benmerah, A., Muntaner, O., Piolot, T., Tramier, M., Coppey-Moisan, M., Bouvier, M., Labbe-Jullie, C., and Marullo, S. (2005) Homo- and hetero-oligomerization of β-arrestins in living cells, *J. Biol. Chem. 280*, 40210−40215.
34. Bunce, C. M., French, P. J., Allen, P., Mountford, J. C., Moor, B., Greaves, M. F., Michell, R. H., and Brown, G. (1993) Comparison of the levels of inositol metabolites in transformed haemopoietic cells and their normal counterparts, *Biochem. J. 289*, 667−673.
35. Sasakawa, N., Sharif, M., and Hanley, M. R. (1995) Metabolism and biological activities of inositol pentakisphosphate and inositol hexakisphosphate, *Biochem. Pharmacol. 50*, 137−146.
36. Shears, S. B. (2001) Assessing the omnipotence of inositol hexakisphosphate, *Cell Signalling 13*, 151−158.
37. Gurevich, V. V., and Benovic, J. L. (2000) Arrestin: Mutagenesis, expression, purification, and functional characterization, *Methods Enzymol. 315*, 422−437.
38. Woodbury, R. L., Hardy, S. J., and Randall, L. L. (2002) Complex behavior in solution of homodimeric SecA, *Protein Sci. 11*, 875−882.
39. Mogridge, J. (2004) Using light scattering to determine the stoichiometry of protein complexes, *Methods Mol. Biol. 261*, 113−118.
40. Gurevich, V. V., Chen, C. Y., Kim, C. M., and Benovic, J. L. (1994) Visual arrestin binding to rhodopsin: Intramolecular interaction between the basic N-terminus and acidic C-terminus of arrestin may regulate binding selectivity, *J. Biol. Chem. 269*, 8721−8727.
41. Lee, S. J., and Montell, C. (2004) Light-dependent translocation of visual arrestin regulated by the NINAC myosin III, *Neuron 43*, 95−103.
42. Wacker, W. B., Donoso, L. A., Kalsow, C. M., Yankeelov, J. A., Jr., and Organisciak, D. T. (1977) Experimental allergic uveitis. Isolation, characterization, and localization of a soluble uveitopathogenic antigen from bovine retina, *J. Immunol. 119*, 1949−1958.
43. Schubert, C., Hirsch, J. A., Gurevich, V. V., Engelman, D. M., Sigler, P. B., and Fleming, K. G. (1999) Visual arrestin activity may be regulated by self-association, *J. Biol. Chem. 274*, 21186−21190.
44. Arshavsky, V. Y. (2003) Protein translocation in photoreceptor light adaptation: A common theme in vertebrate and invertebrate vision, *Sci. STKE PE43*.
45. Xiao, K., McClatchy, D. B., Shukla, A. K., Zhao, Y., Chen, M., Shenoy, S. K., Yates, J. R., III, and Lefkowitz, R. J. (2007) Functional specialization of beta-arrestin interactions revealed by proteomic analysis, *Proc. Natl. Acad. Sci. U.S.A. 104*, 12011−12016.
46. Vishnivetskiy, S. A., Hosey, M. M., Benovic, J. L., and Gurevich, V. V. (2004) Mapping the arrestin−receptor interface: Structural elements responsible for receptor specificity of arrestin proteins, *J. Biol. Chem. 279*, 1262−1268.
47. Hanson, S. M., Francis, D. J., Vishnivetskiy, S. A., Kolobova, E. A., Hubbell, W. L., Klug, C. S., and Gurevich, V. V. (2006) Differential interaction of spin labeled arrestin with inactive and active phosphorhodopsin, *Proc. Natl. Acad. Sci. U.S.A. 103*, 4900−4905.
48. Hanson, S. M., and Gurevich, V. V. (2006) The differential engagement of arrestin surface charges by the various functional forms of the receptor, *J. Biol. Chem. 281*, 3458−3462.
49. Gurevich, V. V., Dion, S. B., Onorato, J. J., Ptasienski, J., Kim, C. M., Sterne-Marr, R., Hosey, M. M., and Benovic, J. L. (1995) Arrestin interaction with G protein-coupled receptors. Direct binding studies of wild type and mutant arrestins with rhodopsin, β2-adrenergic, and m2 muscarinic cholinergic receptors, *J. Biol. Chem. 270*, 720−731.
50. Osawa, S., Raman, D., and Weiss, E. R. (2000) Heterologous expression and reconstitution of rhodopsin with rhodopsin kinase and arrestin, *Methods Enzymol. 315*, 411−422.

BI7021359